

HYPERFINE STRUCTURE MEASUREMENTS OF NEUTRAL MANGANESE WITH FOURIER TRANSFORM SPECTROSCOPY

RICHARD J. BLACKWELL-WHITEHEAD, JULIET C. PICKERING, AND OWEN PEARSE
Blackett Laboratory, Imperial College, London, SW7 2BW, UK; r.blackwell@imperial.ac.uk,
j.pickering@imperial.ac.uk, owen.pearse@imperial.ac.uk

AND

GILLIAN NAVE
National Institute of Standards and Technology, Gaithersburg, MD 20899; gillian.nave@nist.gov
Received 2004 October 6; accepted 2004 December 7

ABSTRACT

We report experimental hyperfine structure constants of levels in the neutral manganese atom, measured using Fourier transform spectroscopy of hollow cathode discharges. In total, 208 spectral lines of astrophysical interest have been analyzed to obtain hyperfine structure constants for 106 levels in Mn I, of which 67 have no previous hyperfine structure measurements. The uncertainties in the magnetic dipole constants, A , are between 1×10^{-4} and $5 \times 10^{-4} \text{ cm}^{-1}$. Hyperfine structure constants for an additional 18 levels compiled from the literature are also given.

Subject headings: atomic data — line: profiles — methods: laboratory

1. INTRODUCTION

A number of new satellite-borne and ground-based spectrographs on telescopes can now fully resolve many features in stellar spectra. In addition to the basic atomic data of wavelength and oscillator strength, the analysis of astrophysical spectra requires information on line broadening effects such as hyperfine structure (HFS), isotope shifts, and Zeeman effects. Such effects cause the line profile to increase in width and the peak intensity of the line to decrease. The line will also appear asymmetric and will no longer be described by a simple Voigt profile. Failure to account for such effects will result in the incorrect measurement of the wavelength and a miscalculation of the equivalent width measured in stellar spectra. This can lead to an incorrect calculation of the abundance of Mn in stars. For example, Jomaron et al. (1999) showed that the abundance of Mn in HgMn stars is overestimated by 2 to 3 orders of magnitude if HFS is not taken into account and, even if a crude estimate of the HFS is made, the derived abundance can be overestimated by a factor of 4. The major component of uncertainty in their estimated abundance was the lack of accurate laboratory HFS measurements. As a result, synthetic spectra from stellar atmospheric models that fail to take into account such line broadening effects show a marked deviation from observation (Kurucz 1993).

In this paper we present new measurements of the magnetic dipole splitting constants, A , and electric quadrupole splitting constants, B , for levels in neutral manganese. More than half of the Mn I levels give rise to strong observed transitions in the solar spectrum (Moore et al. 1966), and an accurate measurement of these HFS constants would be a great aid to stellar analysis. Lines of Mn I are even stronger in HgMn stars, where the abundance of Mn can exceed that of Fe. In total, 56 of the 124 levels presented in this paper have previous laboratory HFS measurements. A small number of these measurements were high-resolution laser measurements with an uncertainty of $\pm 5 \times 10^{-5} \text{ cm}^{-1}$, but the majority used lower resolution techniques and have uncertainties as large as $\pm 300 \times 10^{-5} \text{ cm}^{-1}$.

Our new measurements cover the wavelength range 1913 Å to 5.1 μm ($52,250$ to 1956 cm^{-1}), with an uncertainty between 1×10^{-4} and $5 \times 10^{-4} \text{ cm}^{-1}$. They are part of a more extensive analysis of the Mn I spectrum (Blackwell-Whitehead 2003). The wavelengths and energy levels are being published separately (R. J. Blackwell-Whitehead et al. 2005a, in preparation), as are new measurements on Mn I oscillator strengths (R. J. Blackwell-Whitehead et al. 2005b, in preparation).

2. PREVIOUS WORK ON THE HYPERFINE STRUCTURE IN Mn I

Two significant early experimental hyperfine structure measurements in Mn I were reported by White & Ritschl (1930) and Fisher & Peck (1939) using optical spectroscopy. They measured A constants for 35 levels in the $3d^5 4s(^7S)nl$, $3d^5 4s(^5S)nl$ and $3d^6(^5S)nl$ configurations, with uncertainties between 0.001 and 0.005 cm^{-1} . Since these early papers there have been publications by the following authors: Murakawa (1955), Woodgate & Martin (1957), Rottmann (1958), Walther (1962), Davis et al. (1971), and Luc & Gerstenkorn (1972). The accuracy of these measurements and their application to astrophysics was discussed in a paper by Beynon (1977). The work by Davis et al. (1971) produced the most accurate measurements so far on the ground state of Mn I, $3d^5 4s^2 a^6 S_{5/2}$. Since Beynon's review paper, high-resolution measurements of HFS have been made by Dembczyński et al. (1979), Johann et al. (1981), Kronfeldt et al. (1985), Brodzinski et al. (1987), and Başar et al. (2003) using laser techniques, and by Blackwell-Whitehead (2003) and Lefébvre et al. (2003) using Fourier transform (FT) spectroscopy. The HFS measurements by Blackwell-Whitehead (2003) are included in the current paper.

In the recent HFS measurements by Başar et al. (2003) several of the levels were found to have a nonzero value for the quadrupole constant B . However, the value of the quadrupole constants are an order of magnitude smaller than the dipole constants and are of the same order as the uncertainty in the measurement. For the majority of the levels presented in this

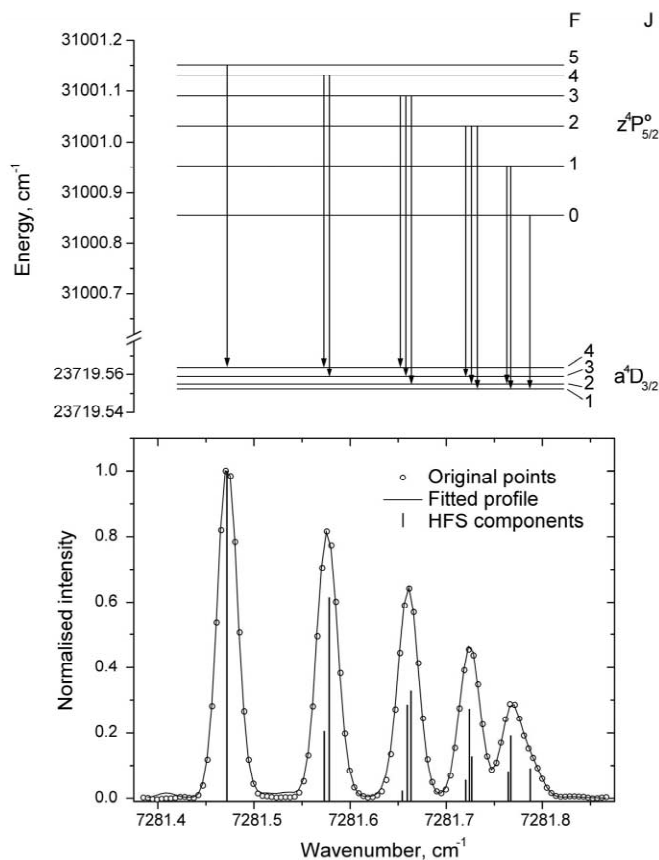


FIG. 1.—HFS profile of the transition $3d^6(^5D)4s a^4D_{3/2} - 3d^5(^6S)4s4p(^3P) z^4P_{5/2}$, as seen in the infrared FT spectrum.

paper, the quadrupole constants were found to be zero to within the uncertainty of our measurements.

3. EXPERIMENTAL PROCEDURE

Three spectrometers were used to record the Mn I spectrum. The region from 1913 Å to 8437 Å ($52,274$ to $11,849$ cm^{-1}) was recorded with the Imperial College (IC) ultraviolet FT spectrometer (Thorne et al. 1987) and the IC vacuum ultraviolet FT spectrometer (Thorne 1996). Spectra were recorded with a resolution of 0.04 to 0.055 cm^{-1} , which is sufficient to fully resolve the Doppler broadened line profiles of the transitions. The infrared (IR) and visible regions from 3333 Å to 5.5 μm (1800 to $30,000$ cm^{-1}) were recorded at the National Institute of Standards and Technology (NIST) with the NIST 2 m FT spectrometer (Nave et al. 1997) using resolutions of 0.008 to 0.03 cm^{-1} .

A water-cooled hollow cathode lamp (HCL) was used as a source for the manganese spectra (Learner & Thorne 1988; Danzmann et al. 1988). Owing to the brittle nature of pure manganese, the cathodes were made of an alloy of 88% Mn and 12% Ni for the IC measurements, and an alloy of 95% Mn and 5% Cu for the NIST measurements. The hollow cathode was run at a current of 500 mA, with 90 Pa of Ar or 340 Pa of Ne as a buffer gas. The HCL discharge was more stable with a Ne buffer gas and gave spectra with a better signal-to-noise ratio.

One of the advantages of measuring the Mn I spectrum over such a broad wavenumber range is that it allows the observation of many transitions to and from a given energy level. This redundancy reduces the possibility that blending from unknown lines will affect the results, and it increases the accuracy of the measurements. For example, the HFS constants for the level

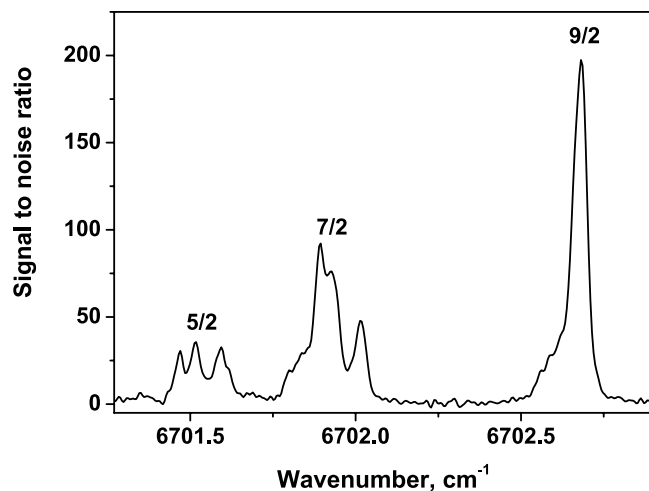


FIG. 2.—Section of the Mn I FT spectrum showing the transitions $5/2 = y^8P_{7/2}^o - f^8D_{5/2}$, $7/2 = y^8P_{7/2}^o - f^8D_{7/2}$, and $9/2 = y^8P_{7/2}^o - f^8D_{9/2}$.

$3d^54s(^7S)5p w^6P_{3/2}^o$ have been measured by analysis of transitions at 6378.343 cm^{-1} ($15,678.05$ Å) and $47,782.353$ cm^{-1} (2092.823 Å).

4. HYPERFINE STRUCTURE ANALYSIS

Manganese has only one stable isotope, ^{55}Mn , but that isotope has an odd number of nucleons with a nuclear magnetic moment of 3.4687 nuclear magnetons and electric quadrupole moment of 0.32 barns (0.32×10^{-28} m^2) (Lide 2003). The interaction of this magnetic moment with the electron field splits the energy levels into the smaller of $2J + 1$ or $2I + 1$ components, where I is the spin of the nucleus ($5/2$ in manganese). In the absence of perturbations the energy of a HFS level is

$$W_F = W_J + \frac{1}{2}AK + B \frac{(3/4)K(K+1) - J(J+1)I(I+1)}{2I(2I-1)J(2J-1)}, \quad (1)$$

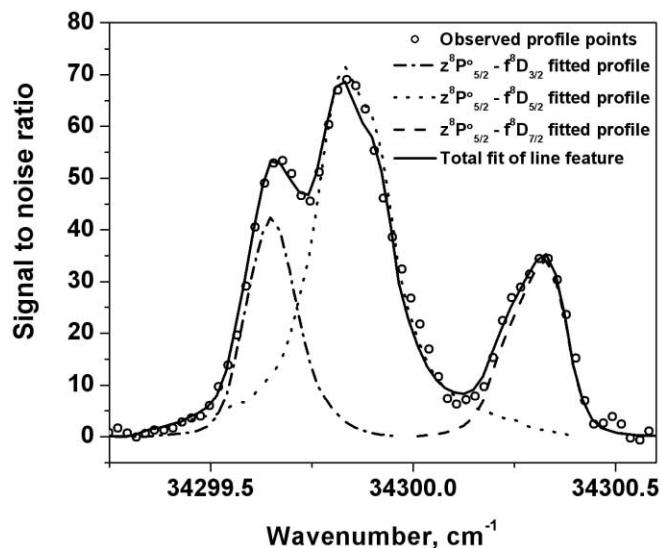


FIG. 3.—Section of the FT spectrum of Mn I showing the calculated line profiles of the $z^8P_{5/2}^o - f^8D_{3/2}$, $-f^8D_{5/2}$ and $-f^8D_{7/2}$ transitions.

TABLE 1
NEW AND REMEASURED HYPERFINE STRUCTURE CONSTANTS FOR EVEN LEVELS IN Mn I

Configuration (1)	Term (2)	J (3)	Energy (cm ⁻¹) (4)	Number of Lines ^a (5)	A^b (10 ⁻³ cm ⁻¹) (6)	B^b (10 ⁻³ cm ⁻¹) (7)	A_{prev}^b (10 ⁻³ cm ⁻¹) (8)	B_{prev}^b (10 ⁻³ cm ⁻¹) (9)	Reference ^c (10)
3d ⁵ 4s ²	a^6S	2.5	0.00		-2.41569 ^d	0.00063 ^d	1
3d ⁶ (⁵ D)4s.....	a^6D	4.5	17052.29		17.02 ± 0.27	4.41 ± 4.00	2
		3.5	17282.00		15.31 ± 0.10	0.72 ± 1.33	2
		2.5	17451.52		14.57 ± 0.10	-1.56 ± 1.00	2
		1.5	17568.48		15.66 ± 0.23	-2.17 ± 1.67	2
		0.5	17637.15		29.42 ± 0.40	...	2
3d ⁶ (⁵ D)4s.....	a^4D	3.5	23296.67	2(4)	-5.4 ± 0.1	...	-5.5 ± 0.3	...	3
		2.5	23549.20	3(5)	-4.6 ± 0.1	...	-4.7 ± 0.2	...	3
		1.5	23719.52	5(7)	1.7 ± 0.2	...	0.9 ± 0.4	...	3
		0.5	23818.87	3(5)	50.6 ± 0.3	...	50.4 ± 0.9	...	3
3d ⁵ 4s ²	a^4G	5.5	25265.74		13.518 ± 0.001	...	4
		2.5	25281.04		19.886 ± 0.001	...	4
		4.5	25285.43		13.182 ± 0.001	...	4
		3.5	25287.74		14.579 ± 0.001	...	4
3d ⁵ 4s ²	a^4P	2.5	27201.54	5(5)	3.0 ± 0.5
		1.5	27248.00	4(4)	7.9 ± 0.5
		0.5	27281.85	3(3)	-19.5 ± 0.5
3d ⁵ 4s ²	b^4D	3.5	30354.21	3(3)	7.8 ± 0.3
		0.5	30411.74	1(1)	43.0 ± 0.4
		2.5	30419.61	7(7)	9.6 ± 0.2	...	9.61 ± 0.17	4.34 ± 1.67	5
		1.5	30425.71	4(4)	14.9 ± 0.4	...	15.21 ± 0.17	-1.27 ± 0.83	5
3d ⁶ (³ H)4s.....	a^4H	6.5	34138.88	5(6)	20.7 ± 0.3
		5.5	34250.52	5(6)	17.2 ± 0.4
		4.5	34343.90	4(5)	13.3 ± 0.5
		3.5	34423.27	6(6)	5.3 ± 0.3
3d ⁶ (³ F ₂)4s.....	a^4F	4.5	34938.70	1(2)	21.5 ± 0.2	...	21.5 ± 0.2	6.7 ± 3.7	5
		3.5	35041.37	1(2)	18.7 ± 0.2	...	19.4 ± 0.4	5.1 ± 1.5	5
		2.5	35114.98	1(2)	14.9 ± 0.3	...	14.6 ± 0.2	0.6 ± 2.8	5
		1.5	35165.05	1(1)	8.0 ± 0.6
3d ⁵ 4s(⁷ S)5s.....	e^8S	3.5	39431.31		24.61 ± 0.09	1.6 ± 1.5	6
3d ⁵ 4s(⁷ S)5s.....	e^6S	2.5	41403.93		26.97 ± 0.01	0.0 (fixed)	6
3d ⁵ 4s(⁷ S)4d.....	e^8D	1.5	46706.09	1(1)	38.4 ± 0.5	...	39 ± 4	...	3
		2.5	46707.03	1(2)	24.1 ± 0.5	...	22 ± 2	...	3
		3.5	46708.33	3(4)	17.6 ± 0.5	...	19 ± 2	...	3
		4.5	46710.15	2(3)	15.7 ± 0.5	...	15 ± 1	...	3
		5.5	46712.58	1(2)	14.5 ± 0.5	...	14.0 ± 0.8	...	3
3d ⁵ 4s(⁷ S)6s.....	f^8S	3.5	50157.63	6(8)	23.2 ± 0.1	7
3d ⁷	e^4P	2.5	51638.17	2(4)	-0.5 ± 0.3	-2.6 ± 2.1
		1.5	51718.22	3(6)	1.9 ± 0.3	2.0 ± 2.0
		0.5	51787.92	1(2)	-13.7 ± 0.4	0.0 ± 1.0
3d ⁵ 4s(⁷ S)5d.....	f^8D	1.5	52702.23 ^f	1(2)	54.7 ± 3.5 ^e	7
		2.5	52702.41 ^f	2(4)	18.4 ± 1.5 ^e	7
		3.5	52702.79 ^f	5(7)	17.1 ± 1.0	7
		4.5	52703.10	4(7)	16.2 ± 0.6	7
		5.5	52705.23	2(3)	14.5 ± 0.4	7

^a The number of lines used to determine the HFS constants. In parentheses are the total number of measurements of these lines in spectra using Ar and Ne as a buffer gas.

^b The uncertainties are 1 standard deviation.

^c Values of A_{prev} and B_{prev} are taken from the reference given in the table.

^d Uncertainty of 1 : 10⁶.

^e Dipole constant A derived from a blended feature.

^f The $f^8D_{7/2,5/2,3/2}$ levels were unresolved in Sugar & Corliss (1985). The values given are preliminary values based on our FT spectra.

REFERENCES.—(1) Davis et al. 1971; (2) Dembczyński et al. 1979; (3) Lefévre et al. 2003; (4) Johann et al. 1981; (5) Başar et al. 2003; (6) Brodzinski et al. 1987; (7) Blackwell-Whitehead 2003.

where W_J is the energy of the fine-structure level of quantum number J ; A and B are the magnetic dipole and the electric quadrupole hyperfine interaction constants, respectively; and K is defined as

$$K = F(F + 1) - J(J + 1) - I(I + 1), \quad (2)$$

where F is the quantum number associated with the total angular momentum of the atom:

$$\mathbf{F} = \mathbf{I} + \mathbf{J}. \quad (3)$$

The majority of the spectral lines in Mn I display observable HFS, and for some of the spectral lines the HFS is quite pronounced. If one of the levels has large dipole constant and the other has a very small dipole constant, the line profile forms a “flag” pattern as seen in Figure 1. In most cases the HFS components are not so regularly spaced and the line profile can take many asymmetric forms.

The interferograms from the FT spectrometer were transformed and phase corrected with the program Xgremlin (Nave et al. 1997), which was also used to determine the dipole and quadrupole constants A and B . The Xgremlin program incorporates the HFS fitting routines of Pulliam (1977) to fit up to three transitions to a spectral feature. There are eight parameters that may be either fixed or allowed to vary: A and B of the upper and lower levels, the center of gravity (CG) wavenumber of the line, the peak intensity of the strongest HFS component, the full width at half-maximum (FWHM) of the HFS components, and the ratio of the Lorentzian width to the total width. Initial values of these parameters for each transition are either estimated or obtained from previous measurements. The program then refines these values with an iterative least-squares fit.

Figures 2 and 3 show an example of the fit of well-separated and heavily blended features in the Mn spectrum. In both cases the lines are due to transitions from the $3d^5 4s(7S)5d f^8 D$ term of which only the $f^8 D_{11/2,9/2}$ levels had been resolved in previous work (Sugar & Corliss 1985). Figure 2 shows three features due to the transitions $f^8 D_{9/2,7/2,5/2} - 3d^5 4s(7S)5p y^8 P_{7/2}^o$, which are well-resolved in our FT spectra. Fitting the HFS of these three transitions, together with similar transitions to the $y^8 P_{5/2}^o$ and $y^8 P_{9/2}^o$ levels, gives dipole constants with uncertainties of between 4×10^{-4} and $1.5 \times 10^{-3} \text{ cm}^{-1}$. However, the $f^8 D_{3/2}$ level can only be determined from two heavily blended transitions near 6720 and 34,300 cm^{-1} . Of these, the one at 34,300 cm^{-1} is less heavily blended and thus gives a more accurate value for the energy level and dipole constant, even though the Doppler broadening is much larger in the ultraviolet region. Figure 3 shows a fit of three transitions to this feature. By fixing the positions and hyperfine components of the two other transitions it was possible to obtain a dipole constant and energy for the $f^8 D_{3/2}$ level. However, the uncertainty is greater than the uncertainties of the other $f^8 D$ dipole constants because of the blending.

The uncertainty in the dipole constants depends on a number of factors. The principal component of uncertainty is the calculated position of the HFS transition components. For weak transitions with a S/N < 10, the wavenumber uncertainty can be large because some component lines may fall below the noise level. However, the uncertainty decreases considerably as the S/N increases. The ratio between the HFS line width and the HFS line separation is also an important factor in determining the uncertainty. A line profile with separately resolved compo-

nents has a lower uncertainty than a profile with blended components or features from another transition. In practice, several different transitions are used to measure the dipole constant for a single level, and the final value is a weighted average of the values determined from the line profile fits. The weighting factor is based on the S/N of the individual line fits such that the average dipole constant A_{av} is given by

$$A_{\text{av}} = \frac{S/N_1}{\sum_k S/N_k} A_1 + \frac{S/N_2}{\sum_k S/N_k} A_2 + \dots + \frac{S/N_N}{\sum_k S/N_k} A_N, \quad (4)$$

where N is the total number of measurements for a particular level. The uncertainty in the dipole constant, ΔA_{av} , is determined from the standard deviation of the individual values:

$$\Delta A_{\text{av}} = \sqrt{\frac{\sum (A_i - A_{\text{av}})^2}{N - 1}}. \quad (5)$$

The resulting uncertainties are similar to those obtained from the uncertainty in the fitted parameters. Where there is only one measurement for a particular level the uncertainty is determined from the uncertainty in the parameters determined using Xgremlin.

For the majority of the lines measured in the new analysis it was found that including the quadrupole constants B of the levels did not alter the fit of the line profile beyond the uncertainty of the calculation. For a small number of the levels, [e.g., $3d^7 e^4 P_j$ and $3d^5(4G)4s4p(^3P) y^4 F_j^o$] the quadrupole constant was of the same order as the dipole constant and the quadrupole constants for these levels are given in Tables 1 and 2.

5. RESULTS

The new experimental HFS constants of even-parity levels of Mn I are presented in Table 1 and those of odd-parity levels in Table 2. We have concentrated on levels that give strong identified lines in solar and stellar spectra (Wallace et al. 1993, 1998; Livingston & Wallace 1991), but for which previous data for HFS constants is either inaccurate or unavailable. In total, 208 spectral lines were measured and the profiles fitted to obtain the hyperfine structure constants for 106 levels. Duplicate measurements of a line were made, where possible, in spectra recorded in both Ar and Ne buffer gases in order to account for possible blends. The total number of line profiles measured was 337. The theoretical calculations of Beynon (1977) of the HFS of levels in the $3d^5 4s(7S)ns$ configurations suggest that some of the HFS levels deviate from the Landé interval rule. The effect is expected to be smaller than our uncertainty and we have not observed it in any of our measurements.

The first three columns of Tables 1 and 2 give the configuration, term and J -value of the energy level. Column (4) gives the energy of the level, taken from Sugar & Corliss (1985). Our experimental value for the dipole constant A is given in column (6), with the estimated uncertainty (1 standard deviation). Column (7) contains our experimental quadrupole constants B with the uncertainty. Columns (8) and (9) give the best previously measured values for the HFS constants, together with the reference in column (10). If two separate measurements have been published of comparable uncertainty, then both references are given. These columns include 18 levels that were not measured by us but that we have used in our fitting procedure to derive HFS constants for

TABLE 2
NEW AND REWORKED HYPERFINE STRUCTURE CONSTANTS FOR ODD LEVELS IN Mn I

Configuration (1)	Term (2)	J (3)	Energy (cm^{-1}) (4)	Number of Lines ^a (5)	A^b (10^{-3} cm^{-1}) (6)	B^b (10^{-3} cm^{-1}) (7)	A_{prev}^b (10^{-3} cm^{-1}) (8)	B_{prev}^b (10^{-3} cm^{-1}) (9)	Reference ^c (10)
$3d^5(^6S)4s4p(^3P)$	z^8P^o	2.5	18402.46	19.08 ± 0.05	0.9 ± 0.4	6
		3.5	18531.64	18.23 ± 0.03	-3.4 ± 0.5	6
		4.5	18705.37	15.22 ± 0.12	1.6 ± 0.9	6
$3d^5(^6S)4s4p(^3P)$	z^4P^o	2.5	31001.15	-20.27 ± 0.05	2.5 ± 5.0	6
		1.5	31076.42	-27.08 ± 0.10	-1.3 ± 1.0	6
		0.5	31124.95	-71.08 ± 0.18	...	6
$3d^6(^5D)4p$	z^6D^o	4.5	41789.48	1(2)	2.9 ± 0.1	...	3.1 ± 0.1	...	3
		3.5	41932.64	3(4)	1.3 ± 0.1	...	1.4 ± 0.2	...	3
		2.5	42053.73	3(5)	-0.9 ± 0.1	...	-8.3 ± 0.5	...	3
		1.5	42143.57	3(4)	-5.0 ± 0.2	...	-4.7 ± 0.2	...	3
		0.5	42198.56	2(3)	-27.4 ± 0.3	...	-26.3 ± 0.4	...	3
$3d^6(^5D)4p$	z^4F^o	4.5	44288.76	1(2)	4.4 ± 0.3	...	4.5 ± 0.5	...	3
		3.5	44523.45	2(4)	5.7 ± 0.2	...	6.0 ± 0.4	...	3
		2.5	44696.29	3(5)	9.5 ± 0.2	...	9.9 ± 0.4	...	3
		1.5	44814.73	3(6)	22.3 ± 0.3	...	22.4 ± 0.9	...	3
$3d^6(^5D)4p$	x^6P^o	3.5	44993.92	4(6)	9.4 ± 0.1	...	9.1 ± 0.3	...	3
		2.5	45156.11	4(5)	9.7 ± 0.1	...	8.7 ± 0.9	...	3
		1.5	45259.17	4(5)	12.5 ± 0.3	...	12 ± 2	...	3
$3d^6(^5D)4p$	z^4D^o	3.5	45754.27	1(2)	1.5 ± 0.4	...	1.53 ± 0.33	4.50 ± 3.50	5
		2.5	45940.93	2(2)	3.1 ± 0.4	...	2.73 ± 0.50	1.00 ± 0.67	5
		1.5	46083.89	2(3)	6.4 ± 0.2	...	6.40 ± 0.17	-0.20 ± 1.67	5
		0.5	46169.93	1(2)	35.6 ± 0.3	...	35.0 ± 0.5	...	3
$3d^54s(^7S)5p$	y^8P^o	2.5	45981.44	1(2)	27.5 ± 0.1	...	27.5 ± 1.5	...	8
		3.5	46000.77	1(2)	20.7 ± 0.1	...	20.0 ± 1.5	...	8
		4.5	46026.75	1(2)	17.3 ± 0.1	...	16.5 ± 1.5	...	8
$3d^6(^5D)4p$	y^4P^o	2.5	46901.13	3(5)	-0.9 ± 0.3	...	-1.8 ± 0.4	...	3
		1.5	47154.51	3(6)	-9.8 ± 0.2	7
		0.5	47299.29	2(4)	-32.5 ± 0.3	...	-34 ± 2	...	3
$3d^54s(^7S)5p$	w^6P^o	3.5	47387.62	2(4)	19.3 ± 0.1	7
		2.5	47659.52	2(4)	25.4 ± 0.2	7
		1.5	47782.43	2(4)	21.6 ± 0.2	7
$3d^5(^4P)4s4p(^3P)$	y^6D^o	0.5	47452.16	1(2)	36.0 ± 0.3
		1.5	47466.66	1(2)	27.5 ± 0.5
		2.5	47753.99	1(2)	22.4 ± 0.4
		3.5	47774.52	3(4)	21.2 ± 0.2
		4.5	47903.80	2(3)	20.1 ± 0.2
$3d^5(^4G)4s4p(^3P)$	y^6F^o	5.5	48021.43	1(1)	20.0 ± 0.4	7
		4.5	48168.01	1(2)	19.0 ± 0.4	7
		3.5	48225.99	3(3)	17.4 ± 0.3	7
		2.5	48270.91	3(4)	16.0 ± 0.2	7
		1.5	48300.98	3(4)	14.3 ± 0.3	7
		0.5	48318.12	2(3)	2.9 ± 0.3	7
$3d^5(^4P)4s4p(^3P)$	v^6P^o	3.5	49888.01	3(4)	18.7 ± 0.2
		2.5	50012.50	3(4)	19.4 ± 0.2
		1.5	50099.03	3(4)	27.0 ± 0.2
$3d^5(^4G)4s4p(^3P)$	z^4H^o	3.5	50065.46	3(3)	7.7 ± 0.4
		4.5	50072.59	2(3)	13.2 ± 0.3
		5.5	50081.31	2(3)	17.3 ± 0.2
		6.5	50094.60	2(3)	20.2 ± 0.4

TABLE 2—Continued

Configuration (1)	Term (2)	J (3)	Energy (cm^{-1}) (4)	Number of Lines ^a (5)	A^b (10^{-3} cm^{-1}) (6)	B^b (10^{-3} cm^{-1}) (7)	A_{prev}^b (10^{-3} cm^{-1}) (8)	B_{prev}^b (10^{-3} cm^{-1}) (9)	Reference ^c (10)
$3d^5(^4G)4s4p(^3P)$	y^4F^o	4.5	50341.30	1(2)	25.4 ± 0.2	0.5 ± 2.0	25.45 ± 0.10	0.50 ± 6.00	5
		3.5	50359.28	1(2)	22.3 ± 0.2	0.0 ± 2.0	22.88 ± 0.67	6.00 ± 1.00	5
		2.5	50373.23	1(2)	17.5 ± 0.4	6.0 ± 4.0	17.67 ± 0.33	3.34 ± 3.67	5
		1.5	50383.27	1(2)	4.3 ± 0.4	0.6 ± 5.0
$3d^5(^4P)4s4p(^3P)$	x^4P^o	2.5	51305.31	2(2)	36.6 ± 0.5
		1.5	51445.55	1(1)	20.9 ± 0.5
		0.5	51552.78	1(1)	24.2 ± 0.5
$3d^5(^4G)4s4p(^3P)$	z^4G^o	2.5	51515.63	2(2)	8.5 ± 1.0^d
		3.5	51530.61	2(2)	14.4 ± 0.2
		4.5	51546.27	2(2)	18.3 ± 0.1
		5.5	51560.93	2(2)	21.5 ± 0.2
$3d^54s(^5S)5p$	w^4P^o	1.5	55368.66	1(2)	18.5 ± 0.4
		2.5	55406.0	1(2)	15.8 ± 0.3
$3d^6(a^3P)4p$	y^4S^o	1.5	57512.08	3(3)	23.3 ± 0.8^d
$3d^5(^4G)4s4p(^1P)$	y^4G^o	5.5	58075.06	1(1)	7.0 ± 0.4
		4.5	58110.24	1(1)	8.7 ± 0.4
		3.5	58136.69	1(1)	16.2 ± 0.5
		2.5	58159.73	1(1)	29.3 ± 0.5
$3d^6(^3H)4p$	y^4H^o	6.5	58338.67	2(2)	13.0 ± 0.3
		5.5	58427.30	3(3)	13.2 ± 0.3
		4.5	58485.52	3(3)	15.0 ± 0.4
		3.5	58519.90	3(3)	18.6 ± 0.2
$3d^6(^3H)4p$	z^4I^o	6.5	58843.39	1(2)	15.7 ± 0.2
		5.5	58851.49	1(2)	14.0 ± 1.0^c
		7.5	58852.60	1(2)	17.2 ± 0.2
		4.5	58866.66	1(2)	11.9 ± 0.2
$3d^5(^2I)4s4p(^3P)$	y^4I^o	7.5	61204.54	1(2)	17.4 ± 0.2
		4.5	61211.43	1(2)	11.8 ± 0.2
		6.5	61225.55	1(1)	13.5 ± 0.5
		5.5	61225.77	1(2)	14.5 ± 0.3

^a The number of lines used to determine the HFS constants. In parenthesis are the total number of measurements of these lines in spectra using Ar and Ne as a buffer gas.

^b The uncertainties are 1 standard deviation.

^c A_{prev} and B_{prev} are taken from the reference given in the table.

^d Derived from transitions with low S/N (S/N < 20).

^e Derived from a blended feature.

REFERENCES.—(3) Lefèbvre et al. 2003; (5) Bařar et al. 2003; (6) Brodzinski et al. 1987; (7) Blackwell-Whitehead 2003; (8) Meléndez 1999.

other levels. Our measurements agree with these previous measurements within the combined uncertainties.

The IR transitions between the $3d^6(^5D)4s a^4D_{7/2-1/2}$ and $3d^54s(^7S)5p y^8P_{9/2-5/2}^o$ levels are of particular interest for the abundance analysis of metal rich stars (Meléndez 1999). If the HFS is neglected it can lead to errors of the order of 25% in the oscillator strength for even the weaker lines (Booth & Blackwell 1983). Prior to the work of Meléndez (1999), the published dipole constants for the $a^4D_{7/2-1/2}$ levels were measured using photographic plates and had an uncertainty in the dipole constants of 0.002 cm^{-1} . The best previously measured dipole constant for the $3d^6(^5D)4s a^4D_{1/2}$ level (White & Ritschl 1930) was almost a factor of 2 smaller than our value. Meléndez determined the A constants for both terms using solar spectra (Livingston & Wallace 1991). Meléndez noted that

two lines at 15,159.7 and 15,216.9 Å, due to the transitions $3d^54s(^7S)5s e^8S_{7/2-y}^o 8P_{9/2}^o$ and $y^8P_{7/2}^o$, were blended with Fe I lines, potentially affecting the dipole constants for the $y^8P_{7/2,9/2}^o$ levels. Our values agree with those of Meléndez to within the joint uncertainties.

The paper of Bařar et al. (2003) reports theoretical dipole constants for levels in the $3d^54s^2$, $3d^64s$, and $3d^7$ configurations, based on a parametric fit to experimental dipole constants. It can be seen in Table 3 that these values agree with our new measurements to within the combined uncertainty of the experiment and the calculations. However, there are a number of exceptions, most notably for the terms $3d^6(^5D)4s a^4D_j$ and $3d^7 e^4P_j$, which differ by at least 0.0025 cm^{-1} . It is possible that the difference between experiment and theory for the a^4D and the e^4P terms is due to $3d^6nl$ and $3d^5nl'n'l'$ configurations that

TABLE 3
A COMPARISON OF THE HYPERFINE STRUCTURE CONSTANTS REPORTED IN THIS PAPER
AND THOSE CALCULATED BY BAŞAR ET AL. (2003)

Configuration	Term	J	Energy (cm^{-1})	A_{obs} (10^{-3} cm^{-1})	A_{calc} (10^{-3} cm^{-1})	ΔA (10^{-3} cm^{-1})
$3d^6(^5D)4s$	a^4D	3.5	23296.67	-5.4	-7.9	2.5
		2.5	23549.20	-4.6	-8.0	3.4
		1.5	23719.52	1.7	-1.8	3.5
		0.5	23818.87	50.6	55.0	-4.4
$3d^54s^2$	a^4P	2.5	27201.54	3.0	4.5	-1.5
		1.5	27248.00	7.9	8.2	-0.3
		0.5	27281.85	-19.5	-18.6	-0.9
$3d^54s^2$	b^4D	3.5	30354.21	7.8	8.0	-0.2
		0.5	30411.74	43.0	41.3	1.7
		2.5	30419.61	9.6	10.2	-0.6
		1.5	30425.71	14.9	14.8	0.1
$3d^6(^3H)4s$	a^4H	6.5	34138.88	20.7	20.3	0.4
		5.5	34250.52	17.2	17.0	0.2
		4.5	34343.90	13.3	11.9	1.4
		3.5	34423.27	5.3	2.7	2.6
$3d^6(^3F2)4s$	a^4F	4.5	34938.70	21.5	21.7	-0.2
		3.5	35041.37	18.7	19.2	-0.5
		2.5	35114.98	14.9	14.0	0.9
		1.5	35165.05	8.0	-1.9	9.9
$3d^7$	e^4P	2.5	51638.17	-0.5	2.0	-2.5
		1.5	51718.22	1.9	3.6	-1.7
		0.5	51787.92	-13.7	-6.8	-6.9

were not included in the analysis of Başar et al. (2003). In addition, Başar et al. (2003) note that the parameters used to calculate the HFS in the $3d^7 e^4P_j$ levels were based on the parameters used for the $3d^54s^2$ configuration because there are no known experimental HFS values for levels with the $3d^7$ configuration. A renewed theoretical analysis of the Mn I HFS including the new experimental results of the present paper is required.

6. SUMMARY

We have analyzed the HFS of 208 lines of Mn I and used this analysis to derive magnetic dipole and electric quadrupole splitting constants for 106 levels. Of these levels, 67 have no previous laboratory measurements of HFS constants. The uncertainty of the measurements ranges from 1×10^{-4} to $5 \times 10^{-4} \text{ cm}^{-1}$ and is an order of magnitude smaller than previous measurements for some of the levels. The $3d^54s(^7S)5d f^8D_{1/2}$, $f^8D_{3/2}$, and $f^8D_{5/2}$ levels were exceedingly difficult to fit using

the current procedure. As a result, the uncertainty in the HFS constants measured for the $f^8D_{1/2}$, $f^8D_{3/2}$, and $f^8D_{5/2}$ levels ranges from 0.0025 to 0.0035 cm^{-1} .

R. B. W. gratefully acknowledges the Engineering and Physical Sciences Research Council of the UK for his Ph.D. studentship and for funding his visit to NIST. R. B. W. also thanks G. Başar for forwarding a preprint of their publication, and for the private communication of the status of their work. J. C. P. thanks the Royal Society and the Particle Physics and Astronomy Research Council of the UK for their support of this work. O. P. thanks the Royal Society for funding his summer Undergraduate Research Opportunities Program work in the FTS laboratory at Imperial College. Work at NIST was supported in part by the US National Aeronautics and Space Administration under the interagency agreement W-10,255 issued through the Office of Space Science.

REFERENCES

- Başar, G., Başar, G., Acar, G., Öztürk, I. K., & Kröger, S. 2003, Phys. Scr., 67, 476
 Beynon, T. G. R. 1977, A&A, 61, 853
 Blackwell-Whitehead, R. J. 2003, Ph.D. thesis, Imperial College, London
 Booth, A. J., & Blackwell, D. E. 1983, MNRAS, 204, 777
 Brodzinski, T., Kronfeldt, H. D., Kropp, J. R., & Winkler, R. 1987, Z. Phys., 7, 161
 Danzmann, K., Günther, M., Fischer, J., Kock, M., & Kühne, M. 1988, Appl. Opt., 27, 4947
 Davis, S. J., Wright, J. J., & Balling, L. C. 1971, Phys. Rev. A, 3, 1220
 Dembczyński, J., Ertmer, W., Johann, U., Penselin, S., & Stinner, P. 1979, Z. Phys., 291, 207
 Fisher, R. A., & Peck, E. R. 1939, Phys. Rev., 55, 270
 Johann, U., Dembczyński, J., & Ertmer, W. 1981, Z. Phys., 303, 7
 Jomaron, C. M., Dworetsky, M. M., & Allen, C. S. 1999, MNRAS, 303, 555
 Kronfeldt, H. D., Kropp, J. R., Subaric, A., & Winkler, R. 1985, Z. Phys., 322, 349
 Kurucz, R. L. 1993, Phys. Scr., 47, 110
 Learner, R. C. M., & Thorne, A. P. 1988, J. Opt. Soc. Am. B, 5, 2045
 Lefébvre, P. H., Garnir, H. P., & Biémont, E. 2003, A&A, 404, 1153
 Lide, D., ed. 2003, CRC Handbook of Chemistry and Physics (84th ed.; Boca Raton: CRC Press)
 Livingston, W., & Wallace, L. 1991, NSO Tech. Rep., 91-001
 Luc, P., & Gerstenkorn, S. 1972, A&A, 18, 209

- Meléndez, J. 1999, MNRAS, 307, 197
Moore, C. E., Minnaert, M. G. J., & Houtgast, J. 1966, NBS Monograph 61
Murakawa, K. J. 1955, J. Phys. Soc. Japan, 10, 336
Nave, G., Sansonetti, C. J., & Griesmann, U. 1997, in Opt. Soc. Am. Tech. Digest Ser. 3, Fourier Transform Spectroscopy: Methods and Applications (Washington: Opt. Soc. Am.), 38
Pulliam, B. V. 1977, M.S. thesis, Purdue Univ.
Rottmann, H. R. 1958, Z. Phys., 153, 158
Sugar, J., & Corliss, C. 1985, J. Phys. Chem. Ref. Data, 14, 338
Thorne, A. P. 1996, Phys. Scr., 65, 31
Thorne, A. P., Harris, C. J., Wynne-Jones, I., Learner, R. C. M., & Cox, G. 1987, J. Phys. E, 20, 54
Wallace, L., Hinkle, K., & Livingston, W. 1993, NSO Tech. Rep., 93-001
———. 1998, NSO Tech. Rep., 98
Walther, H. 1962, Z. Phys., 170, 507
White, H. E., & Ritschl, R. 1930, Phys. Rev., 35, 1146
Woodgate, G. K., & Martin, J. S. 1957, Proc. Phys. Soc. A, 70, 485